

Co-Precipitation Synthesis of ZNCF Nanoparticle and their Structure, Morphological, and Magnetic Properties Characterization

D. Parajuli, V. K. Vagolu, K. Chandramoli, N. Murali and K. Samatha

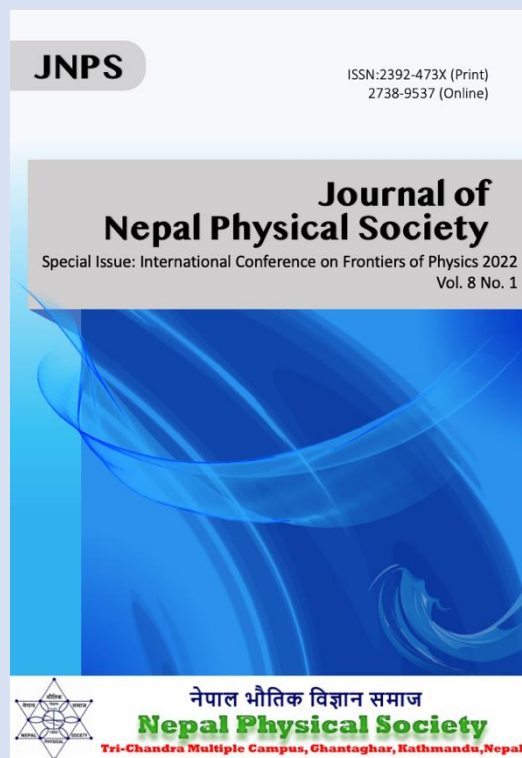
Journal of Nepal Physical Society
Volume 8, No 1, 2022
(Special Issue: ICFP 2022)
ISSN: 2392-473X (Print), 2738-9537 (Online)

Editors:

Dr. Binod Adhikari
Dr. Bhawani Datta Joshi
Dr. Manoj Kumar Yadav
Dr. Krishna Rai
Dr. Rajendra Prasad Adhikari

Managing Editor:

Dr. Nabin Malakar
Worcester State University, MA, USA



JNPS, **8** (1), 22-26 (2022)
DOI: <http://doi.org/10.3126/jnphysoc.v8i1.48281>

Published by: Nepal Physical Society
P.O. Box: 2934
Tri-Chandra Campus
Kathmandu, Nepal
Email: nps.editor@gmail.com



Co-Precipitation Synthesis of ZNCF Nanoparticle and their Structure, Morphological, and Magnetic Properties Characterization

D. Parajuli,^{1,2, a)} V. K. Vagolu,^{3, b)} K. Chandramoli,^{4, c)} N. Murali,^{4, d)} and K. Samatha^{3, e)}

¹⁾Research Center for Applied Science and Technology, Kirtipur, Kathmandu, Nepal

²⁾Tri-Chandra Multiple Campus, Ghantaghar, Kathmandu, Nepal

³⁾Department of Physics, Andhra University, Visakhapatnam-530003, India

⁴⁾Department of Engineering Physics, AUCE, Andhra University, Visakhapatnam-530003, India

^{a)}Corresponding author: deepenparaj@gmail.com

^{b)}Electronic mail: venkatvagolu@gmail.com

^{c)}Electronic mail: kemburu@yahoo.com

^{d)}Electronic mail: muraliphdau@gmail.com

^{e)}Electronic mail: samatha_k2002@yahoo.co.in

Abstract. The Zinc Nickel Cobalt Ferrite (ZNCF) $Zn_{0.95-x}Ni_{0.05}Co_xFe_2O_4$, for $x = 0.01, 0.02, 0.03, 0.04, 0.05$ and 0.06 were prepared by co-precipitation. XRD patterns show spinel ferrite with a cubic structure. The lattice parameter was found to increase linearly with cobalt concentration (x). FESEM gave the grain sizes in the range $1.61-1.38$ nm and particle size in the range $28-21$ nm for $x = 0.01$ to 0.06 . The porosity was in the range $92.6-92.9$ %. The occupancy of metal ions in the two interstitial sites affects the exchange interaction. The higher grain size and lower porosity have a positive impact on magnetic saturation which makes them applicable in recording media.

Received:20 March 2022; Revised:15 April 2022; Accepted:5 May 2022.

Keywords: ZNCF nanoparticles, ferromagnetic spinel, co-precipitation, XRD, FESEM, VSM

INTRODUCTION

The ferrites are highly exploited in recording, medical, fluidity, catalyst, storage, and communication purposes that are activated by magnetic fields. Nickel–Zinc ferrites are soft magnetic materials with high electrical strength and low coercivity, making them a good choice for power transformers in electronic and telecom applications [1]. Co^{2+} , Mg^{2+} , Mn^{2+} , and Cu^{2+} like metal ions can be substituted for Ni–Zn ferrites to change their properties. Their hardness, resistive, chemically stable–like properties made them cheap but highly used for high-frequency purposes. These properties are highly tuned with the cobalt substitution. Cobalt substitution in zinc-nickel ferrite system is highly efficient in electromagnetic wave absorption working in high-frequency conditions [2].

The tunable magnets and compressors [3, 4] radio antenna rods [5], transformers cores, etc. are made by Ni–Co–Zn, Ni–Cu–Zn, Ni–Cd–Zn, Co–Ni–Zn type of ferrites. We have studied varieties of ferrites with different modes with different methods of preparation [6, 7, 8, 9, 10]. The ferrite polycrystalline is used for achieving harder, resistive and stable ferrites. In some cases, soft ferrites are more appropriate for special functions. The cobalt substitution generally lowers the sintering temperature significantly [11]. Lowering the sintering temperature will make the experiment more feasible in most laboratories. The exchange interaction can easily be studied at different frequencies. The cation distribution is obtained at the time of the dielectric and electric properties study. We have recently studied NZCF nanoparticles concerning their structural, morphological, and magnetic properties at room temperature [8].

In this work, we have focused on structural, morphological, and magnetic properties with the use of XRD, FESEM, and VSM respectively.

EXPERIMENTAL PROCEDURE

The co-precipitation method is one of the soft chemical routes which is used for the preparation of the nanoferrites $Zn_{0.95-x}Ni_{0.05}Co_xFe_2O_4$ ($x=0.1,0.2,0.3,0.4,0.5$) with appropriate composition of AR grade aqueous solution in the appropriate ratio of Nickel, Zinc, and Cobalt nitrates against ferric citrate in the equal ratio [11, 12, 13]. This citrate help to make the particles less soluble and decomposes at a lower temperature less than 873 K [14, 15]. Dropwise mixing of ammonium neutral and is dried for 10-12 hours after the addition of ethylene glycol. The puffy and porous precipitation was found which is then dried to get the gel. Self-ignition makes this gel powder which is then calcined at 800°C for 2 hours removing carbon residuals. For the study of magnetic properties, the sample is pressed in the die of 12mm diameter and 2mm thickness with a hydraulic system of 5 tons for 5 minutes. The pallet is then sintered in between 900-1200°C for 2 hrs. Riken BVH-50 VSM was used for its magnetic properties.

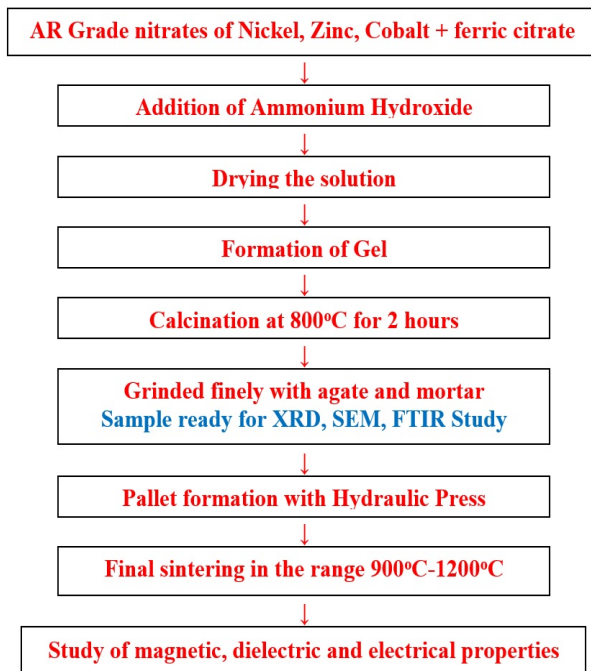


FIGURE 1. Preparation of the ZNCF samples by Co-precipitation method.



FIGURE 2. Puffy and porous ZNCF samples obtained after co-precipitation.

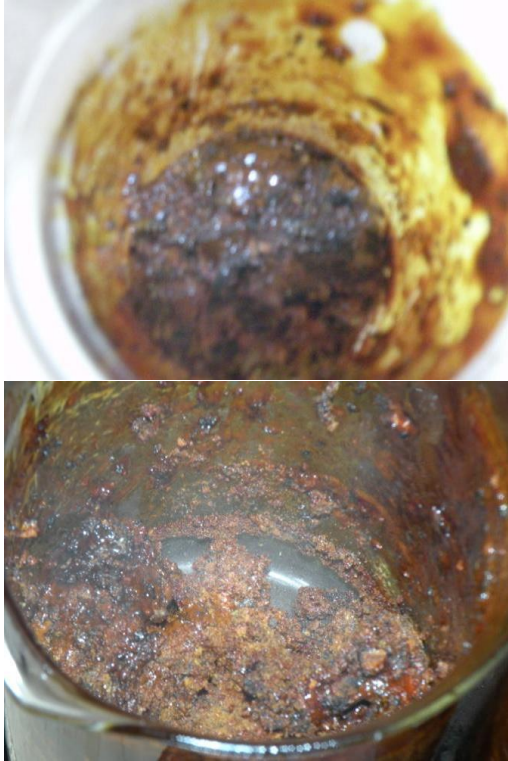


FIGURE 3. Puffy and porous ZNCF samples obtained after co-precipitation.

RESULT AND DISCUSSION

X-ray Diffraction (XRD) Study

The XRD patterns $Zn_{0.95-x}Ni_{0.05}Co_xFe_2O_4$ (ZNCF) samples are shown in figure 2. The highest peak is at the 311 plane and other peaks are at (111), (220), (311), (222), (400), (422), (511), and (440) planes. The pattern matches JCPDS file No. 08-0234 indicating their pure spinel ferrite with cubic structure [16].

The lattice constant was calculated using

$$a = d\sqrt{(h^2 + k^2 + l^2)} \quad (1)$$

where h, k, and l are the Miller indices of the crystal planes and d is the inter-planar distance for the hkl planes. An increase in the lattice constant was observed with an increase in the zinc doping concentration due to the comparable sizes of Co^{2+} (0.78 Å) and Zn^{2+} (0.83 Å), thus the influence of the zinc concentration on the lattice constant depicted in FIGURE 3 followed Vegard's law [17, 18]. Debye-Scherrer's formula was used to calculate the average crystallite size of the samples:

$$D = 0.89\lambda / \beta \cos\theta \quad (2)$$

Where λ is the incident wavelength of the Cu $K\alpha$ radiation for the XRD, β is the full width at half maximum (FWHM) in radians on the 2θ scale, θ is Bragg's angle, and D is the crystallite size in nm. The crystallite size of the samples increased due to the replacement of the smaller radius Co^{2+} ions with larger-radius Zn^{2+} ions.

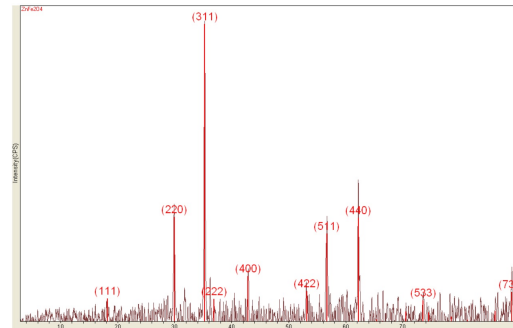


FIGURE 4. X-ray diffraction pattern of Zinc ferrite

Field Emission Scanning Electron Microscope (FESEM) study

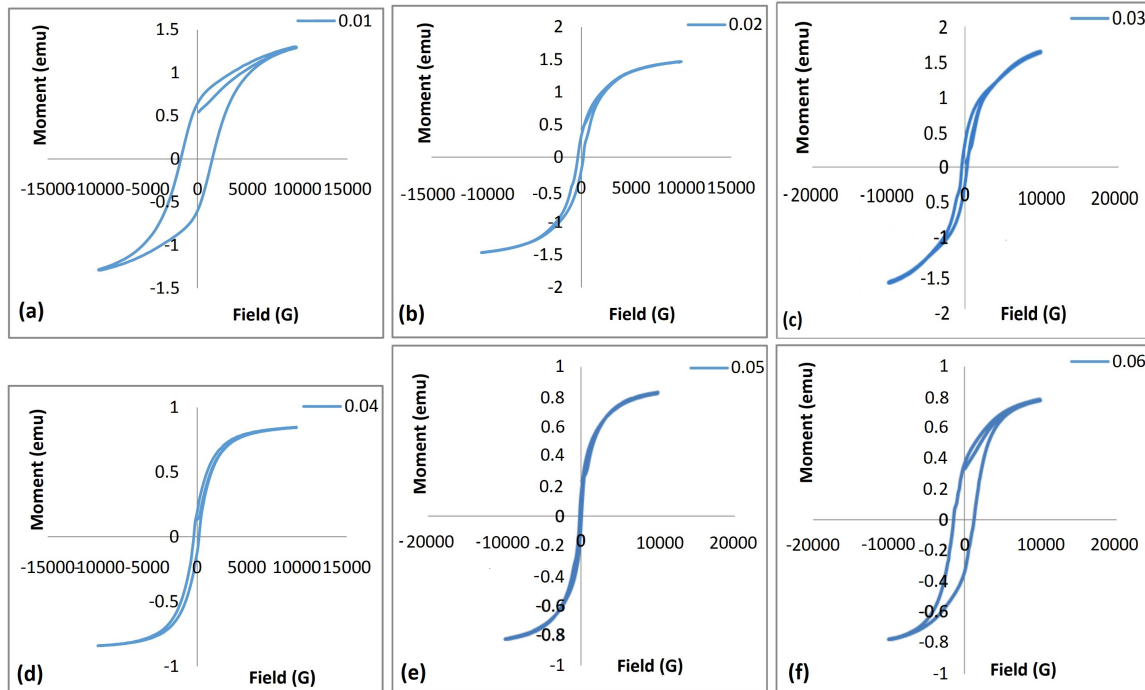
The microstructures of the $Zn_{0.95-x}Ni_{0.05}Co_xFe_2O_4$ ($x=0.1, 0.2, 0.3, 0.4, 0.5$) obtained from FESEM are as shown in Figure 3 (a-f). The different structural and morphological data obtained are listed in Table 1. The average grain size obtained from the line intercept method was found to be in the wider range of 1.61-1.38nm than that of NZCF [16]. Similarly, the particle size was found in the narrower range of 28-21 nm with a nearly spherical shape. They are agglomerated at higher sintering temperatures. The density percentage is in the narrower range of 92.6-92.9 %. The porosity is in the range of 7.1-7.9%. The data obtained are appropriate for recording media.

Vibrating Sample Magnetometer (VSM) Study

The magnetic saturation (M_s), magnetic remanence (M_r), and coercivity (H_c) of the cobalt substituted Zinc-Nickel ferrites at room temperature are calculated from the hysteresis loops as shown in Figure 4(a) to 3(f) respectively for (a) 0.01 (b) 0.02 (c) 0.03 (d) 0.04 (e) 0.05 (f) 0.06. The M_s is decreasing with cobalt concentration due to the interaction of metallic cations in the interstitial sites A and B [8, 19]. The magnetic anisotropy and magnetic moment created are due to the orbitals of Co^{2+} ions. The nonmagnetic nature of Oxygen ions makes the two

TABLE I. Structural variation of ZNCF

S.N.	Sample	Lattice Parameter	Density(%)	FWHM	Porosity	Grain size (D nm)	Particle size (nm)
1.	0.01	8.387	92.6	0.279	7.1	1.61	28
2.	0.02	8.389	91.4	0.276	7.0	1.60	27
3.	0.03	8.392	91.7	0.232	6.1	1.52	22
4.	0.04	8.395	90.9	0.255	7.8	1.45	22
5.	0.05	8.396	92.5	0.271	8.1	1.40	21
6.	0.06	8.398	92.9	0.275	7.9	1.38	21

**FIGURE 5.** FESEM microstructure of $Zn_{0.95-x}Ni_{0.05}Co_xFe_2O_4$ for $x =$ (a) 0.01 (b) 0.02 (c) 0.03 (d) 0.04 (e) 0.05 (f) 0.06

magnetic ions apart in the ferrite lattice thereby creating the superexchange correlation between those magnetic and non-magnetic ions. This led to the super-exchange interaction among the magnetic ions with neighboring nonmagnetic ions. However, the vacancy created in the absence of oxygen on the surface might be occupied by the impurity ions thereby creating the spin disorder that breaks the exchange among the magnetic ions [20]. The ferrite is pure. Instead, the value of M_s is decreased.

The first decreasing and increasing pattern is seen in the coercivity with the amount of cobalt as shown in Figure 4 for ZNCF. Coercivity is directly proportional to the magnetocrystalline anisotropy constant which is the result of the spin-orbit coupling due to the Co^{2+} ions. The domain wall is then decreased showing the superparamagnetic particles in totality. In addition, the coercivity is reduced due to the grains behaving as the magnetic dipole due to magnetic saturation which is degraded with the porosity in the lattices [3]. On the other hand, the Zn^{2+} ions enter-

ing the $Co_xFe_2O_4$ spinel lattice might have caused the disappearance of the spin-orbit coupling, which determines the magnetic anisotropy in the nanocrystalline ferrites. Hence, the addition of Zn^{2+} into the $Co_xFe_2O_4$ spinel lattice decreased the magnetic anisotropy, which increased the domain wall energy resulting in a decrease in the H_c of the ZNCF samples with increasing x from 0 to 1.0. This variation in M_s and H_c values can be attributed to the difference in cation distribution in the ZNCF samples [21]. In addition, the spin canting and size effect in the ZNCF samples could have affected the magnetic properties. According to the reported results, the ZNCF displayed an antiferromagnetic behavior with a normal spinel structure $(Zn^{2+})Td[Fe^{3+}Fe^{3+}]OhO^{2-}_4$ within which all of the Zn^{2+} cations were located at the tetrahedral [A] sites and the Fe^{3+} cations were at the octahedral [B] sites with antiparallel moments [22]. Thereby, the substitution of nonmagnetic ions with a preferential [A] site occupancy resulted in a reduction in the exchange interactions be-

tween the [A] and [B] sites. Hence, it is possible to change the magnetic properties of ZNCF by varying the degree of zinc substitution. In general, the chemical composition, cation distribution, structure, grain size, defects, and internal strain can influence the magnetic properties of spinel ferrites. In short, the superparamagnetic property is seen in $(\text{Zn}^{2+})\text{Td}[\text{Fe}^{3+}\text{Fe}^{3+}]\text{OhO}^{2-}_4$ with the medium concentration of the cobalt under consideration.

CONCLUSION

The $\text{Zn}_{0.95-x}\text{Ni}_{0.05}\text{Co}_x\text{Fe}_2\text{O}_4$ for $x = 0.01, 0.02, 0.03, 0.04, 0.05$ and 0.06 were successfully synthesized with the co-precipitation method. The XRD patterns show their spinel structure with ferrimagnetic nature. On increasing the cobalt concentration, the values of lattice parameter a (Å) raise due to the higher ionic radii of the substituents. The magnetic saturation (M_s) decreases with cobalt content showing superparamagnetic nature. FESEM gave the grain sizes in the range $1.61\text{--}1.38\text{nm}$ and particle size in the range $28\text{--}21\text{ nm}$ for $x = 0.01$ to 0.06 . The porosity was in the range $92.6\text{--}92.9\%$. The properties investigated in this work show sufficient index for high-density recording media and other allied applications.

EDITORS' NOTE

This manuscript was submitted to the Association of Nepali Physicists in America (ANPA) Conference 2021 for publication in the special issue of Journal of Nepal Physical Society.

REFERENCES

1. K. V. Kumar, D. Paramesh, P. V. Reddy, *et al.*, "Effect of aluminium doping on structural and magnetic properties of ni-zn ferrite nanoparticles," *World Journal of Nano Science and Engineering* **5**, 68 (2015).
2. J. Y. S. D H Kang and J. H. Oh, "The microwave absorbing characteristics nizco of ferrite composite microwave absorber," *Proceedings of the ICF* **6**, 30 (1992).
3. R. Shinde, H. Bhasin, and M. Karmarkar, "7th int. conf. on ferrites (bordeaux, france)," *J. Phys. IV France* **7**, C1–149 (1997).
4. R. Y. C. R.S. Shinde, P. Pareek, "Nickel zinc ferrite materials for pulsed applications in accelerators," .
5. F. N. Bradley, "Materials for magnetic functions," (1971).
6. D. Parajuli and K. Samatha, "Structural analysis of cu substituted ni\zn in ni-zn ferrite," *Bibechana* **18**, 128–133 (2021).
7. D. Parajuli and K. Samatha, "Morphological analysis of cu substituted ni\zn in ni-zn ferrites," *BIBECHANA* **18**, 80–86 (2021).
8. D. Parajuli, V. Vagolu, K. Chandramoli, N. Murali, and K. Samatha, "Soft chemical synthesis of nickel-zinc-cobalt-ferrite nanoparticles and their structural, morphological and magnetic study at room temperature," *Journal of Nepal Physical Society* **7**, 14–18 (2021).
9. D. Parajuli, N. Murali, and K. Samatha, "Structural, morphological, and magnetic properties of nickel substituted cobalt zinc nanoferrites at different sintering temperature," *Journal of Nepal Physical Society* **7**, 24–32 (2021).
10. D. Parajuli, P. Tadesse, N. Murali, and K. Samatha, "Correlation between the structural, magnetic, and dc resistivity properties of co0. 5m0. 5-xcuxfe2o4 (m= mg, and zn) nano ferrites," *Applied Physics A* **128**, 1–9 (2022).
11. M. Goldberg, T. Obolkina, S. Smirnov, P. Protsenko, D. Titov, O. Antonova, A. Konovalov, E. Kudryavtsev, I. Sviridova, V. Kirsanova, *et al.*, "The influence of co additive on the sintering, mechanical properties, cytocompatibility, and digital light processing based stereolithography of 3y-tzp-5al2o3 ceramics," *Materials* **13**, 2789 (2020).
12. A. L. Stuijts, J. Verweel, and H. Peloschek, "Dense ferrites and their applications," *IEEE Transactions on Communication and Electronics* **83**, 726–736 (1964).
13. P. Reijnen, "Sintering behaviour and microstructures of aluminates and ferrites with spinel structure with regard to deviation from stoichiometry," *Science of Ceramics* **4**, 169–188 (1968).
14. J. Burke, "Kinetics of high temperature processes," *The Technology Press of Massachusetts Institute of Technology and J. Wiley & Sons, Inc., New York Chapman & Hall, Limited, London* , 109–16 (1959).
15. M. PAULUS, "Preparation conditions of the ferrites," in *Preparative Methods in Solid State Chemistry*, edited by P. HAGENMULLER (Academic Press, 1972) pp. 487–531.
16. J. Longo, H. Horowitz, L. Clevenna, S. Holt, J. Milstein, and M. Robbins, "Solid state chemistry-a contemporary overview (advances in chemistry series)," (1986).
17. L. Zhang and S. Li, "Empirical atom model of vegard's law," *Physica B: Condensed Matter* **434**, 38–43 (2014).
18. R. D. Shannon, "Revised effective ionic radii and systematic studies of interatomic distances in halides and chalcogenides," *Acta crystallographica section A: crystal physics, diffraction, theoretical and general crystallography* **32**, 751–767 (1976).
19. B. D. Cullity, *Elements of X-ray Diffraction* (Addison-Wesley Publishing, 1956).
20. R. D. Waldron, "Infrared spectra of ferrites," *Phys. Rev.* **99**, 1727–1735 (1955).
21. O. Kondrat'eva, G. Nikiforova, A. Tyurin, E. Shevchenko, E. Andrusenko, M. Smirnova, V. Ketsko, and K. Gavrichev, "Thermodynamic and magnetic properties of magnesium-gallium ferrite ceramics," *Ceramics International* **44**, 4367–4374 (2018).
22. T. Tatarchuk, M. Bououdina, N. Paliychuk, I. Yaremiy, and V. Moklyak, "Structural characterization and antistructure modeling of cobalt-substituted zinc ferrites," *Journal of Alloys and Compounds* **694**, 777–791 (2017).
23. D. Parajuli, P. Tadesse, N. Murali, and K. Samatha, "Study of structural, electromagnetic and dielectric properties of cadmium substituted ni-zn nanosized ferrites," *Journal of the Indian Chemical Society* **99**, 100380 (2022).